

PREDICTIONS FOR SUSY PARTICLE MASSES FROM ELECTROWEAK BARYOGENESIS

J. M. CLINE

McGill University, Dept. of Physics, 3600 University St., Montréal (Qc) H3A 2T8, Canada
E-mail: jcline@physics.mcgill.ca

In collaboration with G.D. Moore,¹ the electroweak phase transition in the minimal supersymmetric standard model is studied using the two-loop effective potential. We make a comprehensive search of the MSSM parameter space consistent with electroweak baryogenesis, taking into account various factors: the latest experimental constraints on the Higgs boson mass and the ρ parameter, the possibility of significant squark and Higgs boson mixing, and the exact rate of bubble nucleation and sphaleron transitions. Most of the baryogenesis-allowed regions of parameter space will be probed by LEP 200, hence the Higgs boson is likely to be discovered soon if the baryon asymmetry was indeed created during the electroweak phase transition.

1 Introduction

An attractive possibility for explaining the baryon asymmetry of the universe,

$$\frac{n_B - n_{\bar{B}}}{n_\gamma} \sim 10^{-10} \quad (1)$$

is electroweak baryogenesis, combined with supersymmetry. This is one of the only pictures which makes fairly definite low-energy predictions, which are in effect being tested now at LEP and the Tevatron by their searches for the Higgs boson and the top squark.^{1,2}

Let us review the basic picture of electroweak baryogenesis. It assumes that the electroweak phase transition (EWPT) is strongly first order, hence bubbles of the true vacuum, with nonzero Higgs VEV $\langle H \rangle$, nucleate inside the false vacuum, at a critical temperature T_c near 100 GeV (fig. 1). Outside the bubble, anomalous baryon-violating interactions (sphalerons), present in the Standard Model, are occurring much faster than the Hubble expansion rate. Inside the bubble, if $\langle H \rangle/T_c$ is larger than ~ 1 , these interactions are out of equilibrium. In addition there must be CP-violating interactions at the bubble wall, which cause an asymmetry in the reflection probability for particles versus antiparticles (and left-handed versus right-handed particles) from the wall. This causes a build-up of CP asymmetry in front of the wall, which the sphalerons attempt to erase. But in so doing, they create a baryon asymmetry in front of the wall, which gradually falls behind the wall due to the steady expansion of the latter into the plasma, and collisions of the reflected particles with other particles in the plasma. This baryon excess survives to become the baryonic matter of the present-day universe.

There have been attempts to implement electroweak baryogenesis in other ways, for example, using cosmic strings instead of bubbles. The idea is that $\langle H \rangle$ can be suppressed inside the strings; then strings could work similarly to bubbles except that the baryon (B) violation is going on inside of the strings as they sweep through

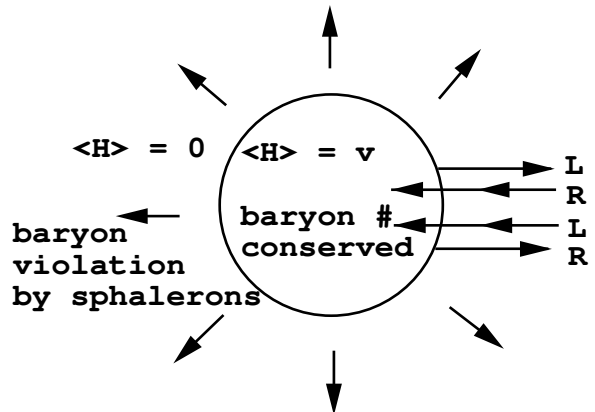


Figure 1: Expanding bubble during the electroweak phase transition. Left-handed fermions reflect into right-handed ones and vice versa, but with different probabilities.

space, while B is conserved outside because the temperature is assumed to be much less than T_c . We have made a quantitative study of all aspects of this proposal³ (except for the possibility of superconducting strings which carry an enormous current), and concluded that it falls short of being able to produce the required B asymmetry by 10 orders of magnitude. One reason for the failure is that the CP violation scales with the string velocity (v) squared, whereas the density of a string network scales like v^{-2} . It is therefore impossible to tune the density to enhance the asymmetry. Another reason for the failure is that sphalerons are typically large compared to strings, and their energy, E_{sph} , is increased if they are squashed so as to fit inside a string. This suppresses their likelihood, hence the rate of B violation, by a Boltzmann factor, $e^{-E_{sph}/T}$.

Thus the expanding bubble picture is the most likely realization of electroweak baryogenesis. And it is also highly constrained, since it is not easy to get a large enough asymmetry. One of the major challenges is in getting the phase transition to be strong enough so that $\langle H \rangle/T_c \geq 1$.

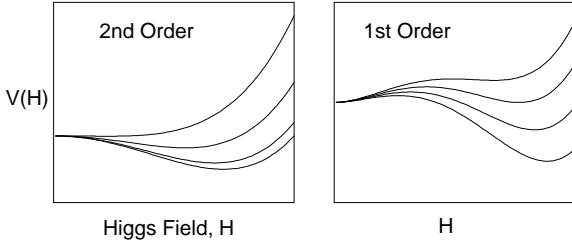


Figure 2: (a) Higgs effective potential for several temperatures, with a second order transition. (b) Same, but with a first order transition.

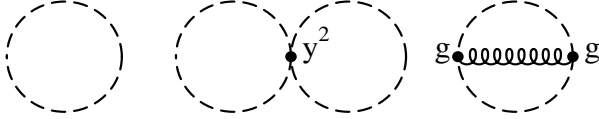


Figure 3: The most important one- and two-loop stop diagrams contributing to the effective potential.

2 Strength of the Phase Transition

In the Standard Model, the EWPT is second order, as illustrated in figure 2a. The effective potential, $V(H)$, never develops a barrier between the high-temperature, symmetric phase minimum ($H = 0$) and the low- T , broken phase one ($H \neq 0$). Bubbles do not form in this case, so baryogenesis as outlined above cannot occur. However, the EWPT can be first order in the Minimal Supersymmetric Standard Model (MSSM) if one of the top squarks (the mostly right-handed one) is sufficiently light^{2,4,5,6} giving an effective potential of the form shown in figure 2b.

In the presence of light stops (light compared to the temperature), $V(H)$ gets finite-temperature contributions from vacuum loop diagrams containing stops and possibly gluons, like those of figure 3. The propagators are evaluated at an arbitrary value of the background Higgs fields, of which there are two in the MSSM. The squark masses appearing in the propagators are the Higgs-field-dependent eigenvalues of the mass matrix

$$\mathcal{M}_t^2 \cong \begin{pmatrix} m_Q^2 + y^2 H_2^2 + O(m_Z^2) & y(A_t H_2 - \mu H_1) \\ y(A_t H_2 - \mu H_1) & m_U^2 + y^2 H_2^2 + O(m_Z^2) \end{pmatrix}. \quad (2)$$

Because the top Yukawa coupling y is large, the stops couple strongly to the Higgs field H_2 , and this is why they have a potentially strong effect on $V(H)$.

We have computed $V(H)$ to two loops, including mixing effects between the stops and between the heavy and light Higgs fields. We then searched the MSSM parameter space to find regions where the phase transition is strong enough for successful baryogenesis, while still

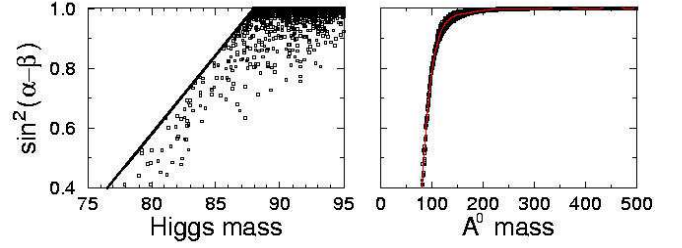


Figure 4: (a) Scatter plot from Monte Carlo in plane of Higgs mixing angles versus lightest Higgs mass (in GeV); (b) Same, but with the mass of the A^0 Higgs boson.

compatible with other experimental constraints.

3 Important Parameters and Constraints

Now I will discuss the parameters which have the strongest effect on the EWPT.

Lightest Higgs mass, m_h . The transition is strongest if m_h is small. Moreover, the light Higgs field h is related to the flavor eigenstates H_i by a mixing angle α ,

$$h = \sin \alpha H_1 + \cos \alpha H_2, \quad (3)$$

and the phase transition is also strongest when $\sin^2(\alpha - \beta) \approx 1$, where $\tan \beta = \langle H_2 \rangle / \langle H_1 \rangle$. This is illustrated in fig. 4a, which shows the distribution of allowed points from our Monte Carlo of the parameter space, in the plane of $\sin^2(\alpha - \beta)$ and m_h . The region to the left of the line is experimentally excluded by LEP.

CP-odd Higgs mass, m_{A^0} . A strong phase transition also favors the pseudoscalar Higgs boson, A^0 , being heavy. In fact, this explains the preference for $\sin^2(\alpha - \beta) \approx 1$, because there is a strong correlation between m_{A^0} and $\sin^2(\alpha - \beta)$, as shown in fig. 4b. In the limit where both become large, the Higgs sector of the MSSM becomes SM-like, with all the heavy Higgs bosons decoupling.

$\tan \beta$ and m_U^2 . We find a lower limit on the value of $\tan \beta$ which gives a strong enough transition:

$$\tan \beta > 2.1 \quad (4)$$

This is coming largely from the fact that m_h depends on $\tan \beta$,

$$m_h^2 = \frac{1}{2} \left[m_A^2 + m_Z^2 - \sqrt{(m_A^2 + m_Z^2)^2 - 4m_Z^2 m_A^2 \cos^2 2\beta} \right] + O \left[(m_t^4/v^2) \ln(m_{\tilde{t}_1} m_{\tilde{t}_2}/m_t^2) \right], \quad (5)$$

in such a way that its tree-level value vanishes when $\tan \beta = 1$. Thus to satisfy the experimental constraints on the Higgs mass, one must take $\tan \beta$ to be greater than

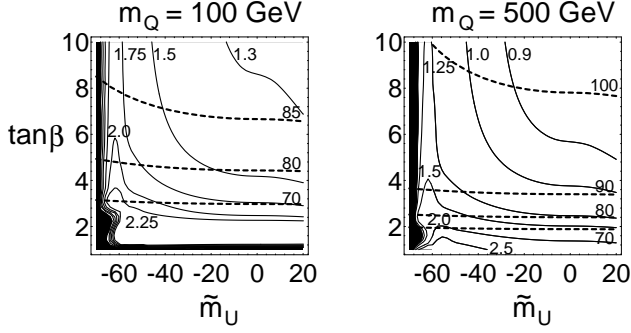


Figure 5: Contours of v/T (solid) and Higgs mass (dashed) in the plane of $\tan\beta$ and $\tilde{m}_U \equiv m_U^2/|m_U|$ (in GeV), for $m_Q = 100$ and 500 GeV, respectively, at zero squark mixing ($\mu = A_t = 0$). The potential has color-breaking minima in the black regions near $\tilde{m}_U = -70$ GeV.

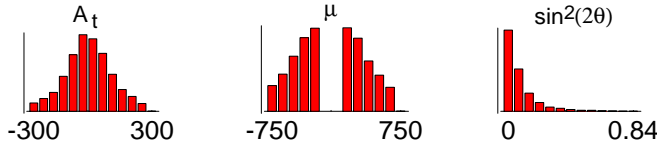


Figure 6: Histograms for squark mixing parameters and mixing angle from Monte Carlo. Mass parameters are in GeV.

some minimum value. As for larger values of $\tan\beta$, these tend to weaken the phase transition. However this effect can be counteracted by enhancing the stop contribution to $V(H)$, *i.e.*, by making the stop lighter. To make the right-handed stop sufficiently light, we must in fact take its mass parameter m_U^2 to be negative! This combines with the term m_t^2 in eq. (2) to give an overall positive mass squared, except before the EWPT when $m_t = 0$. Figure 5 shows how the strength of the phase transition (measured as $\langle H \rangle/T$, where $\langle H \rangle = \sqrt{\langle H_1 \rangle^2 + \langle H_2 \rangle^2}$) depends on $\tan\beta$ and on $\tilde{m}_U \equiv m_U^2/|m_U|$.

Squark mixing parameters, μ and A_t . Although the EWPT is generally stronger for small values of the squark mixing parameters (appearing in the off-diagonal elements of the mass matrix (2)), the preference is rather weak. Histograms for μ , A_t and the squark left-right mixing angle θ are shown in figure 6. Small values of $|\mu|$ are experimentally excluded by chargino and neutralino searches, explaining the absence of points near $\mu = 0$.

Left-handed stop mass. The left-handed stop mass parameter is bounded from below,

$$m_Q > 130 \text{ GeV}. \quad (6)$$

This comes from the requirement that the contributions to the ρ parameter from the squarks not exceed precision electroweak bounds (we take $\Delta\rho < 1.5 \times 10^{-3}$). Because the light Higgs mass depends on m_Q through radiative corrections, it has a noticeable effect on the baryogenesis

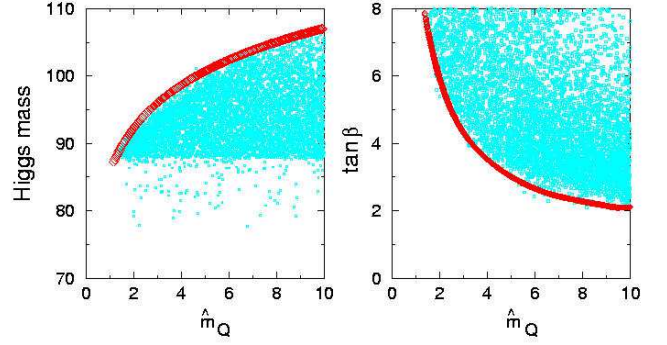


Figure 7: Scatter plots from Monte Carlo for m_h and $\tan\beta$ versus $\hat{m}_Q \equiv m_Q/(100 \text{ GeV})$.

limits on these parameters. The maximum allowed light Higgs mass, and the minimum allowed values of $\tan\beta$, depend on $\hat{m}_Q \equiv (m_Q/100 \text{ GeV})$ as

$$m_h \leq 85.9 + 9.2 \ln(\hat{m}_Q) \text{ GeV} \\ \tan\beta \geq (0.03 + 0.076 \hat{m}_Q - 0.0031 \hat{m}_Q^2)^{-1}. \quad (7)$$

The corresponding scatter plots from the Monte Carlo, for these quantities versus m_Q are shown in figure 7.

4 Strong Phase Transition at Small m_{A^0} ?

We have seen that the majority of accepted points in our Monte Carlo are those with large values of m_{A^0} . There are some rare exceptions, as can be seen in fig. 7a: the sparse points below $m_h = 87$ GeV are those with $m_{A^0} \sim 100$ GeV. Although they infrequently give a strong enough transition, they could be important for the following reason. Most of the contributions to the CP asymmetry that gives baryogenesis are proportional to the amount by which $\tan\beta$ changes inside the bubble wall, and this is strongly correlated with the value of m_{A^0} .

The concept of $\Delta\beta$, the deviation in β , is illustrated in fig. 8. The path in field space taken by the Higgs field as it goes from inside the bubble ($\langle H \rangle > 0$) to outside ($\langle H \rangle = 0$) is shown for the case of $m_{A^0} = \infty$, where it is a straight line, and for $m_{A^0} \sim 100$ GeV, which gives some curvature to the path. The maximum angular deviation from straightness can be called $\Delta\beta$, and computed from the effective potential. (For technical reasons we define $\Delta\beta \equiv \max_v [v(\beta(v) - \beta(v_c))]/v_c$, where v is the value of $\langle H \rangle$ at any point inside the bubble wall.) In figure 9 we show how $\Delta\beta$ is correlated with m_{A^0} and the frequency of $\Delta\beta$ values. Typically $\Delta\beta$ is quite small, 10^{-3} , and only very rarely reaches 10^{-2} , as also found by others.⁷

Since most electroweak baryogenesis mechanisms have $n_B \propto \Delta\beta$, this gives an additional suppression in the

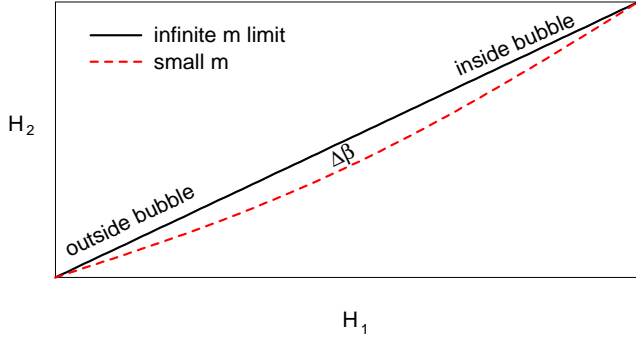


Figure 8: Trajectories in Higgs field space for going through the bubble wall, in the limits of large and small m_{A^0} .

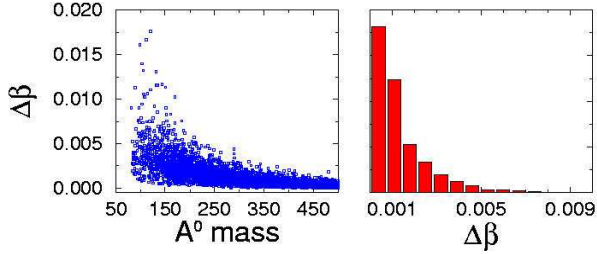


Figure 9: (a) Maximum deviation in weighted Higgs VEV orientation, $\Delta\beta \equiv \max_v [v(\beta(v) - \beta(v_c))]/v_c$, inside bubble wall, as a function of m_{A^0} ; (b) distribution of $\Delta\beta$ values.

baryon asymmetry that can be produced in electroweak mechanisms, which has been overlooked by some authors. Interestingly, there is one contribution to the CP asymmetry which has been shown to be unsuppressed⁸ in the limit of vanishing $\Delta\beta$. Charginos, which have the Dirac mass matrix

$$\mathcal{M}_{\tilde{W}\tilde{h}} = \begin{pmatrix} m_2 & gH_2/\sqrt{2} \\ gH_1/\sqrt{2} & \mu \end{pmatrix}, \quad (8)$$

can experience a CP-violating force while traversing the bubble wall if the μ parameter is complex, even if H_1/H_2 remains constant in the wall.

5 Squark Masses and Mixing

Previous studies of the EWPT have emphasized the weakening effect that squark mixing has on the phase transition strength. We have already pointed out that the Monte Carlo, although favoring small mixing between the left- and right-handed stops, does not strongly exclude large mixing: see figure 6 and eq. (2). Since nonzero values of μ are needed to get CP violation, this is fortunate!

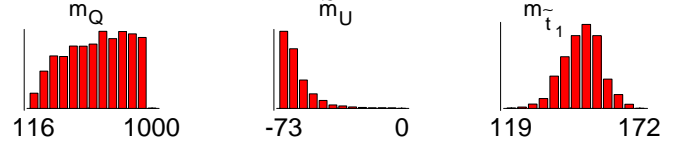


Figure 10: Monte Carlo distributions for the mass parameters of (a) the left stop and (b) the right stop; and (c) the actual mass of the right stop, in GeV.

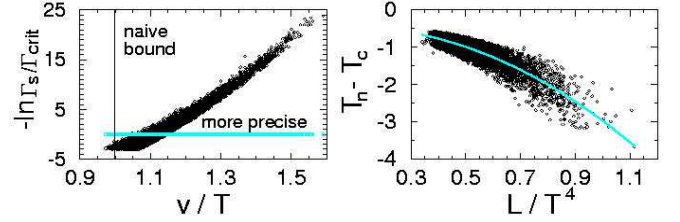


Figure 11: (a) Correlation of the sphaleron rate with v/T ; below the line would be ruled out baryon preservation; (b) $\Delta T \equiv T_n - T_c$ in GeV versus $\Lambda \equiv (\text{latent heat})/T^4$, fit by the function $\Delta T = -0.5 + 0.5\Lambda - 2.9\Lambda^2$.

As for the stop masses, the distributions of the relevant parameters can be seen in figure 10. The left-handed stop (which in the limit of large m_Q has mass approximately equal to m_Q) is usually much heavier than the right-handed one, but can be as light as 116 GeV. The right-handed one is always relatively light, in the range $119 \text{ GeV} < m_{\tilde{t}_1} < 172 \text{ GeV}$. Such a light squark is potentially discoverable at the Tevatron, but this depends strongly on the value of gluino mass, $m_{\tilde{g}}$. The discovery potential is greatly suppressed if $m_{\tilde{g}} > 300 \text{ GeV}$.

6 Sphaleron Rate versus Higgs VEV; Latent Heat

In this work we have also made a detailed study of the exact criterion for a strong enough phase transition. Recall that the requirement is that sphaleron interactions inside the bubbles must be slow enough so that the baryon number produced does not get erased afterwards. The naive condition for fulfilling this is that $\langle H \rangle/T_c \geq 1$, but the more exact criterion is that the rate of sphaleron interactions, Γ_s , must exceed some critical lower value, Γ_{crit} , derived in ref. [1]. By plotting $-\ln \Gamma_s/\Gamma_{crit}$ versus v/T (fig. 11a), we can see how far off the naive condition is. The figure shows that a significant number of trial parameter sets are excluded by the exact bound, although they may pass the $\langle H \rangle/T > 1$ condition. However, we have tried to correct for the fact that the effective potential approach underestimates the strength of the phase transition by about 10%, compared to nonperturbative lattice results.⁶ Because of this, our threshold for accep-

tance is somewhat looser than $\Gamma_s = \Gamma_{crit}$.

We have also studied the issue of reheating after the onset of the phase transition, which is related to the latent heat L . L is defined to be the difference in $dV/d \ln T$ between the symmetric ($\langle H \rangle = 0$) and broken ($\langle H \rangle \neq 0$) phases. Although the phase transition becomes energetically possible starting at the critical temperature T_c , where the two phases are degenerate in energy, stable bubbles do not start to appear until the somewhat lower nucleation temperature, T_n . If the transition is strong enough, entropy production at the bubble walls could conceivably reheat the universe all the way back to T_c . In general the reheat temperature (T_r) is given by

$$\begin{aligned} \frac{T_c - T_r}{T_c - T_n} &= 1 - \frac{30L}{g_* \pi^2 (T_c^4 - T_n^4)} \\ &\cong 1 - \frac{15L}{2g_* \pi^2 T_c^3 (T_c - T_n)}, \end{aligned} \quad (9)$$

which approaches zero if $T_r \rightarrow T_c$ (here g_* is the number of relativistic degrees of freedom in the plasma). We find a correlation between L and $T_c - T_n$ (fig. 11b) so that the right hand side can be thought of as being a function of L alone, roughly. We also find that $(T_c - T_r)/(T_c - T_n)$ is always in the range $[0.6, 0.8]$, so that reheating to T_c is never achieved. One reason to be interested in this is that complete reheating to T_c tends to slow the growth of the bubbles significantly, and most baryogenesis mechanisms predict that the baryon asymmetry is enhanced by $1/v$ if the bubble wall velocity v is small.

7 Will Electroweak Baryogenesis be Ruled Out (or In) by LEP?

The most pressing question confronting electroweak baryogenesis is whether it is really testable at LEP. Fig. 12 shows the regions in the $\tan \beta - m_h$ plane which will be excluded in runs near 200 GeV center of mass energy. At first sight the experimentally inaccessible region $m_h > 95$ GeV, $\tan \beta > 10$ might look worrisome, since these values appear to be allowed by our Monte Carlo. Closer examination shows that these points only escape detection by LEP if m_{A^0} and $\sin^2(\alpha - \beta)$ are too small to be compatible with a strong phase transition. The real worry is whether $m_h > 107$ GeV, which is above the discovery potential of LEP 200, but still compatible with baryogenesis if the left-handed stop is heavy enough. In this case we will have to hope for the slim possibility of the Higgs being discovered at Tevatron.

8 Conclusions

The most promising experimental signal for electroweak baryogenesis is a light Higgs, with $m_h < 86$ GeV if the

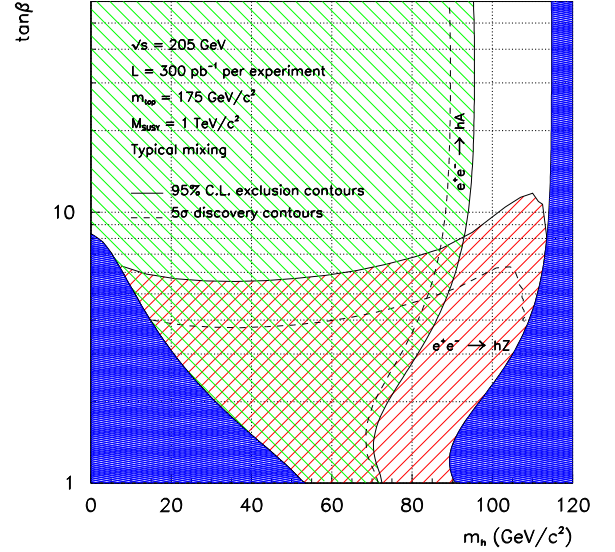


Figure 12: Discovery potential of LEP 2.

left-stop mass parameter m_Q is 100 GeV, and $m_h < 116$ GeV if $m_Q = 2$ TeV. It is also possible that the mostly right-handed top squark will be observed, since its mass is constrained to lie in the range $119 \text{ GeV} < m_{\tilde{t}} < 172 \text{ GeV}$. This extreme lightness of the stop can only be achieved by taking its mass parameter m_U^2 to be dangerously negative. The danger is that the universe will get stuck in a color-breaking minimum with a nonzero stop condensate, and not be able to tunnel into the normal vacuum state where we live. Although it has been previously investigated,⁵ this issue probably deserves closer scrutiny.

References^a

1. J.M. Cline and G.D. Moore, hep-ph/9806354, to appear in Phys. Rev. Lett. (1998).
2. M. Carena, M. Quiros and C.E.M. Wagner, hep-ph/9710401, Nucl. Phys. B524, 3 (1998).
3. J.M. Cline, J.R. Espinosa, G.D. Moore and A. Riotto, preprint hep-ph/9810261 (1998).
4. J.R. Espinosa, , hep-ph/9604320, Nucl. Phys. B475 (1996) 273
5. D. Bödeker, P. John, M. Laine and M.G. Schmidt, hep-ph/9612364, Nucl. Phys. B497 (1997) 387.
6. M. Laine and K. Rummukainen, hep-ph/9804255, Phys. Rev. Lett. 80 (1998) 5259 ; hep-lat/9804019, preprint CERN-TH-98-122 (1998)
7. J.M. Moreno, M. Quiros and M. Seco, hep-ph/9801272, Nucl. Phys. B526 (1998) 489.
8. J.M. Cline, M. Joyce and K. Kainulainen, hep-ph/9708393, Phys. Lett. B417 (1998) 79.

^asee ref. 1 for a more complete list of references.